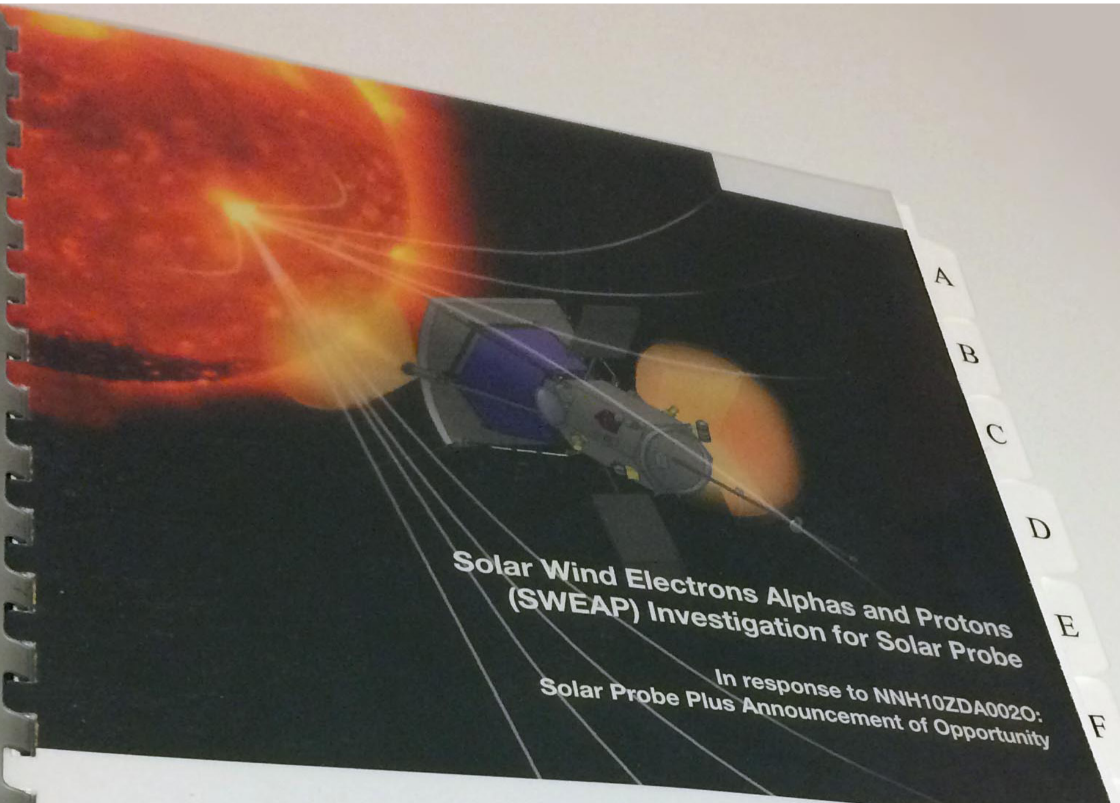

Solar Wind Electrons Alphas and Protons (SWEAP) Investigation for Solar Probe

In response to NNH10ZDA002O:
Solar Probe Plus Announcement of Opportunity

Submitted 26 March 2010

Dr. Justin C. Kasper
Principal Investigator

Mr. Thomas G. Bonnenfant
Contracting Officer
Smithsonian Astrophysical Observatory

Through a contract with a Boston placement agency, Tom Nalesnik joined the staff of the Harvard-Smithsonian Center for Astrophysics in Cambridge, MA. His job: to serve as lead graphic designer and proofreader/editor on a massive, 150-page proposal that the scientists there were putting together for an upcoming NASA space mission.

The project was not a simple one — there were a wide variety of technical materials that had to be incorporated into the proposal, including charts, graphs, illustrations, and photographs, as well as text supplied by the Harvard-Smithsonian Astrophysics Center's team of scientists.

In terms of design, the overall look and page layout had to accommodate a number of different elements, including large multi-page chart foldouts, and a pocket for a CD-ROM containing a digital copy of the NASA proposal.

The result? The Harvard-Smithsonian Center for Astrophysics landed the $67 million, multi-year contract with NASA — and Tom was called back to work on additional proposals for other NASA projects they were bidding on.

the theoretical effort needed to interpret SWEAP measurements and will produce higher order data products. Partners from the Massachusetts Institute of Technology (MIT), Los Alamos National Laboratory (LANL), and NASA Goddard Space Flight Center (GSFC) support the science and the instrument designs.

D.1.2: Background

SPP is a once-in-a-lifetime opportunity to explore the atmosphere of our Star, make unexpected discoveries, and - with the right instruments - bring about fundamental understanding of the physics of the corona and solar wind. Fueled by convection and magnetic fields, the plasma temperature rapidly rises within hundreds of kilometers of the surface of our Sun from the relatively cool 6000K photosphere through a 10000K transition region and gives birth to the 1-10MK solar corona. The hot corona is unstable, producing a supersonic solar wind that pervades interplanetary space and carves the protective heliospheric bubble out of the interstellar medium. While fifty years have passed since the prediction and detection of the solar wind, we still do not understand how the corona is heated and how the solar wind is accelerated. SPP will directly visit the atmosphere of our star and close the observational gap between remote and *in situ* observations of the inner heliosphere.

SPP will challenge our understanding of the solar wind and corona. Our models for the origin of the wind rest on remote observations and *in situ* measurements no closer than 0.3 AU from the Sun. In the modern paradigm, the wind is composed of fast and slow streams interspersed with occasional transient coronal mass ejections (CMEs). The commonly accepted properties of slow, fast, and transient wind in the interplanetary medium are summarized in Table D1.2-1. Slow wind generally exhibits highly variable structure and composition but simple i+ and e- VDFs that are close to Maxwellian and have similar temperatures. Fast wind is less variable, but often has ... fluctuations and rich non-Maxwellian VDFs, including different temperatures, anisotropies, and velocities between ions. These non-Maxwellian properties are believed to be signatures of the wave-particle coupling responsible for the ... speed and mass flux of the fast wind. By ... within 9.5 solar radii (R_s) of the Sun, SPP ... directly probe the solar wind as it emerges ... the corona and establish direct connections between the wind and source regions on the ... SPP is also very likely to produce ... simple analysis of solar wind at 1 AU ... how our current paradigm (Table D1.2-1) ... distorted by our biased view from ... (Kasper et al., 2008). Fig. D1.2-1 shows ... tribution of the temperature ratio and ... flow between alphas and protons as a ... of speed (left panel) and collisional age ... Coulomb collision frequency multiplied ... transit time of the wind from the Sun ... We see that low A_c is a much better ... non-Maxwellian features than solar wind ... Slow wind, with a longer transit time ... er collision rate washes out these ... wave-particle processes, suggesting ... ics will be revealed by SPP ... *This hints at the surprises that we ...*

Table D1.2-1: The standard picture of the *in situ* solar wind, divided into fast and slow steady state solar wind and transient coronal mass ejections (CMEs).

Category/Characteristic	Slow Wind	Fast Wind
Likely sources	Streamer belt, active regions, coronal hole boundary layers	Coronal holes, active regions
Typical speeds	< 400 km/s	700 - 900 km/s
Temperatures	$T_p < Te$	$T_p > Te$
VDFs	Nearly Maxwellian, equal temperatures	Highly nonthermal with anisotropies, differential flow, and beams, mass-proportional temperatures
	Filamentary, highly variable	Uniform, slow changes
Signature	... fractionation ... iable	Coronal He/H ~ 5%, steady

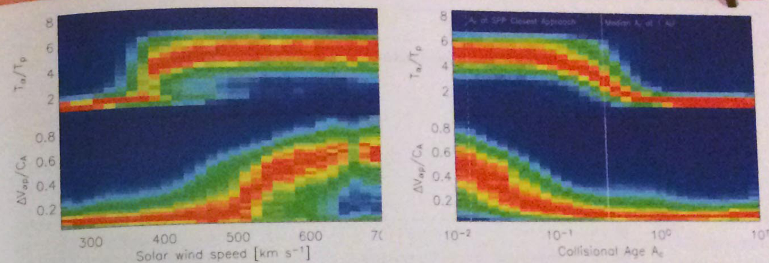

***Figure D1.2-1**: Distribution of the temperature ratio (T_α/T_p) of alphas to protons and the differential flow between the species normalized by the Alfvén speed ($\Delta V_{\alpha p}/C_A$) as function of solar wind speed (left) and collisional age A_c (right) using the same set of four million Wind/FC observations. A smaller number of collisions during propagation to Earth seem to be more important than speed in determining if the plasma will be non-Maxwellian. Vertical lines indicate the median value of Ac at 1 AU (solid) and at 9.5_{Rs} (dashed), suggesting SPP may discover that all wind is non-Maxwellian near the Sun.*

with SPP and suggests that we should not take our current understanding of the basic solar wind, its origin and properties, as established.

SWEAP science goals and measurement requirements developed in the following section were supported by an extensive analysis of models and observations. Fig. D1.2-2 summarizes some characteristic speeds and temporal scales that SPP will encounter as a function of distance from the Sun. Simulations of the radial dependence of fast solar wind from a coronal hole and slow wind from active regions and the streamer belt were compared with extrapolations of Helios observations from 0.3-1 AU and remote coronal diagnostics for consistency to produce our best guess of solar wind conditions. These predictions guide the science goals and measurement requirements established in D.1.2. Where possible we have designed SWEAP to detect not only the average expected range of critical parameters but also the extremes.

For ease of evaluation of SWEAP in the context of SPP and other instrument proposals we have followed the organizational structure of the goals outlined in the STDT. Sections D.1.2.1 through D.1.2.4 present the SPP Objectives and SWEAP goals, and are highlighted in the same color used in the traceability matrix in Foldout 1 (FO1).

D.1.2.1: Sources of the Solar Wind

SPP Objective 1: Determine the structure and dynamics of the magnetic fields at the sources of the fast and slow solar wind

SWEAP provides the data products and coverage required to identify the location and physics of solar wind sources. Robotic exploration of the heliosphere has produced fifty years of *in situ* solar wind measurements. These data, combined with remote solar and coronal imaging and spectroscopy, shape our understanding of the global magnetic and plasma connections from the surface of the Sun through interplanetary space. By associating solar wind speeds, composition, temperature, and non-Maxwellian properties with coronal features we discover the sources regions of the solar wind: fast wind associated with coronal holes, slow wind emerging either from the streamer belt or active regions, and coronal mass ejections (CMEs) producing transient solar wind at all speeds. SPP and SWEAP will allow us to move from discovery of solar wind sources to understanding the underlying physics: How do these source regions map into the heliosphere, and what fraction of the corona is actually magnetically open to the heliosphere at any instant in time and over the solar cycle? If slow wind emerges from the streamer belt, how does it extend to such a large range in latitude? What fraction of small-scale structures in the interplanetary medium, from magnetic holes and reconnection exhausts to density fluctuations and magnetic discontinuities, are signatures of coronal physics or features that develop within the solar wind during propagation?

1.1: Connect the large scale structure of the solar wind to solar sources. Fundamental questions remain about solar wind source regions, especially for the slow wind. What fraction of the slow solar wind, if any, emerges from the streamer belt, from active regions, and from the boundaries of front of the instrument if properly shielded. Materials at these high temperatures can evaporate, sputter, and outgas, especially when the plasma is factored in, leading to changes in thermal/optical properties and degrading performance. Any instrument that uses Sun-exposed materials at high voltages must also tolerate e- emission due to both the hot cathode and field effect mechanisms. The SWEAP team worked with specialists in laboratory plasmas, nuclear reactor design, and aerospace vehicle surfaces to identify the optimum but standard materials that could survive and operate in these conditions. We chose to avoid the use of any thermo-optical surface treatments to remove uncertainty due to degradation over the mission lifetime. For the conducting grids within SPC, we found the best materials to withstand the harsh conditions are high purity tungsten (W) and Silicon-Carbide (SiC) crystal grown through the chemical vapor deposition (CVD) process. W has a high work function and the highest melting temperature of the refractory metals. CVD SiC is one of the strongest materials on Earth and can be doped to make it a conductor. Titanium and alumina are also ideal materials.

SPC grids can easily survive the highest temperatures and plasma fluxes. Both SPP and SPC will be exposed to a novel environment, with surfaces experiencing high temperatures, plasma fluxes, and more than 500 times the solar intensity at 1 AU. The most important demonstration for SPC was to prove that a conducting grid could survive these conditions. We used the Processes, Materials and Solar Energy (PROMES) laboratory in Perpignan, France to conduct these tests. PROMES features the largest solar furnace in the world (Fig. E1.2-1). The furnace focuses up to 1 MW of sunlight onto the entrance to a quartz-windowed vacuum chamber. The chamber includes a particle accelerator that can reproduce solar wind ion fluxes, a UV light source to reproduce the portion of the solar spectrum blocked by the atmosphere, and diagnostic equipment to monitor mass loss and surface temperatures. A W grid was imaged with a scanning electron microscope (SEM), placed in the chamber and heated beyond 1400C by sunlight, and then removed and re-imaged. The SEM images in Fig. E1.2-1 show that the grid survived the exposure with no degradation. In fact, smoothing of grain boundaries increased the reflectivity of the grid by 50%, improving its thermal performance. Later that year W samples at the furnace were raised to 2500C and simultaneously exposed to an ion beam four orders of magnitude more intense than the solar wind at 9.5 R_s, also reporting no damage.

The SWEAP team has designed, manufactured, and operated a prototype of the SPC sensor. A detailed mechanical, electrical, and thermal design (Described in E.1.2.3) was developed based on the performance requirements established in D.1.2 and FO1. The prototype was then built, verifying manufacturability of the design and the time and level of effort required to assemble the sensor. Fig. E1.2-2 shows a photograph of the FSU from the front. Performance of the prototype at room temperature was verified in a solar wind facility at MSFC. The current produced by a constant energy beam was measured as a function of the voltage applied to the HV grid. Many aspects of the design must be correct for the current to drop sharply when the HV surpasses the beam energy. The plot in the figure shows the cutoff for protons using a SiC grid, showing a cutoff with a width of about 2%, typical for the FCs we have developed in the past and sufficient to produce the needed accuracy in density, temperature, and velocity. In Phase B we will conduct similar tests of SPC in the MSFC facility but heated to encounter temperatures to demonstrate instrument performance in the full SPP environment.

Figure E1.2-1: *The PI at PROMES conducting SPC tests in 2008 (left). SEM image of W grid before (middle) and after (right) exposure showing no affect other than improvement in surface reflectance.*

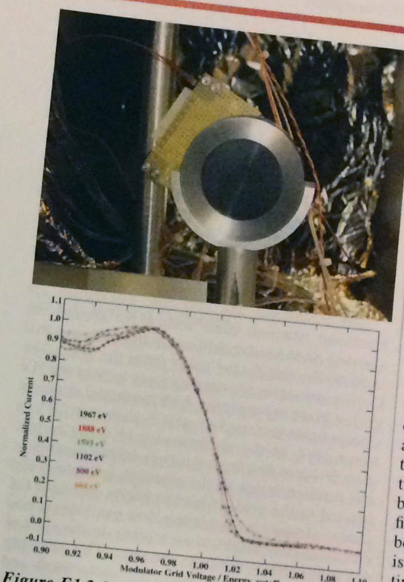

Figure E1.2-2: *Top: A full-sized prototype of the SPC sensor was completed in 2010 and demonstrated in the MSFC solar wind facility with protons and e- beams and W and SiC grids. Bottom: Measured proton current (at six beam energies) as a function of the ratio of the voltage in the instrument to the beam energy demonstrating successful energy resolution.*

E.1.2.3: Design

Overview of SPC components. SPC was designed following standard practices for solar wind FCs but with certain mechanical parts replaced with components made from standard materials more appropriate for higher temperatures. SPC is divided into several smaller units, which are described here, in the nomenclature tree on FO2, and at the component level in the Master Equipment List (MEL) in J.7. The FC Sensor Unit (FSU) is the actual FC sensor that is exposed to sunlight. Three annular titanium plates at the front of the FSU permit plasma to flow into the instrument while shielding the edges of the SPC from sunlight. The FSU is mounted on the end of the FC Strut Unit (FTU), whi
strut that runs along the SPP tr
and interfaces SPC to the SW
Module (SWEM) on the SPP b
distributions within the FSU and
in FO3 in F. High Voltage (HV
generated by the HV Modulato
in SWEM and transmitted inside
FSU. The currents from the plates
by pre-amplifiers housed within
lated FC Proximity Module (FP
near the FSU but within the shad
heat shield. The conditioned signa
ted from the FPM down the FTU
Processing Board (APB) in the
they are digitized.

A schematic of the FSU is sho
E1.2-3. The larger modulator assem
filters particles by energy/charge ar
collector assembly on the right rec
and flow angles of the particles.
the FSU through the large circular e
ture on the left and enters the modu
bly. The entrance aperture is design
ficiently large that the smaller limit
between the modulator and collecto
is always fully illuminated by plasma
tire range of angles of incidence.
aperture is sized to detect the minimu
high signal to noise, including the dr
strength due to the transparency of the
dimensions of the FSU are directly de
the desired sensitivity (8 mm diamet
aperture for high signal to noise detecti
wind from 9.5 Rs to 0.25 AU), range
able flow angles (50 mm diameter entra
vide full response over an 80° FOV) a
range (modulator sized to withstand
25% margin).

Fine conducting grids with high tran
throughout both assemblies act to filter
and shield stray electric fields. Previ
have used woven W wire meshes epoxied
rings for the grids. Since the epoxy w
survive SPC operating temperatures, w
replaced the wire meshes with monolith
from single wafers of high purity W and S
E.3.3.2). The W grid is created with a w
etch and the SiC grid is created through
ma etch process. Both grid types were ma
tured and tested in pre-Phase A developmen
have found that these new grids are signifi
stronger and more suitable for FCs than th
wire meshes, which were prone to failure thr

Description	Sub	Breadbo	Mass M	Eng. M	Qual. M	Flight M	Flight Sp	Mass Pr	Random V	Sine Vibr	Bakeou	Elevated Te	TVAc & Cyclin	Thermal Balanc
Suite/Payload														
SWEAP Suite	S				1	1								
Instrument														
Solar Probe Cup (SPC)	I			1	1	1								
Solar Probe Analyzer (SPAN)	I				1	1								
Module														
Faraday Cup Module (FCM)	M		1	1	1	1			F	F	F			
Faraday Cup Prox Module (FPM)	M		1	1	1	1							QF	
SPAN-A Instrument Module	M		1		1	1			QF	QF	QF			
SPAN-B Instrument Module	M		1		1	1			QF	QF	QF		QF	
SWEAP Elec Module (SWEM)	M		1	1	1	1			QF	QF	QF		QF	
Unit														
FCM Sensor Unit (FSU)	U	2		1	2[4]	1	1	M	QF	QF				
FCM Strut Unit (FTU)	U			1	1	1	1	M	Q	Q		Q	QF	
FCM Cable Unit (FCU)	U	1		1	1	1	1	M			F		QF	
FPM Electronics Unit (FEU)	U	1		1	1	1	1	M	QF	QF				
FPM Cable Unit (FPCU)	U	1		1	1	1	1	M			F		QF	
SPAN-A Sensor Unit (ASU)	U				1	1	1	M						
SPAN-A Cable Unit (ACU)	U				1	1	1	M			F			
SPAN-B Sensor Unit (BSU)	U				1	1	1	M						
SPAN-B Cable Unit (BCU)	U				1	1	1	M			F			
SWEM Electronics Box Unit (SWEB)	U				1	1		M						
SWEM Electrical Cabling Unit (SWEC)	U				1	1		M			F			
Assembly														
SWEB Low-Volt Pwr Supply Board	A				1	1	1						QF	
SWEB Analog Processor Board (APB)	A	1			1	1	1						QF	
SWEB High-Voltage Mod Board (HMB)	A	1			1	1	1						QF	
SWEB Digital Control Board (DCB)	A				1	1	1						QF	

- Responsibility Legend: SAO · UCB · MSFC
- Verification Method: Q= Qualification Test on QM or EM; P=Protoflight Test on FM; F=Acceptance Te...
- Notes: 1 = An electrostatically clean design will be implemented
  2 = Radiation tolerant parts will be selected
  3 = A functional test for the appropriate asembly level will be performed after each environm...
  4 = A separate thermal qualification model is being made specifically for high temperature te...

Panel and TSA strut), flexured SPC mechanical interface permits SPC to interface to the spacecraft bus, as required by the AO. Implementation of the associated trade study (Sect. F.3.7.2) to a single-point, TSA strut interface would reduce SWEAP mass and reduce the mechanical complexity of our interface to SPP.

SPC Thermal. A single-point SPP/SPC interface holds a thermal advantage over the proposed two-point interface. The single-point interface would not impact adjacent SPP radiators in terms of viewing the long FTU strut at elevated temperature.

Electrostatic and Magnetic Cleanliness. We will work with the spacecraft provider to ensure that S/C-generated ...ectric and magnetic fields do not interfere with low-en... ...urements, and that the space-

craft does not charg...
Data Exchang... ...ates autonom... the spacecraft. S... netic field, sp... gers. We coul... other instrum...
SWEAP p... the solar w... to rotate at ... the need for ... discussed in ... spacecraft p... operational ... tion of SW...

SWEAP Implement...

Foldout 3 (FO3)

A Telemetry Resource Summary

Element	CBE	Cont.	Total
	bps	[%]	bps
SWEAP data rate to SPP DPU	23.544	27%	29.995
Contingency from reducing burst data from 60 to 30 mins/day			
Total Suite Telemetry Resources	**23.544**	**27%**	**29.995**

B Mass Resource Summary

Element	CBE	Cont.	Total
	[kg]	[%]	[kg]
SPC Instrument	**2.591**	**32%**	**3.414**
Thermal Heat Shield Assy	0.136	30%	0.177
Modulator Assembly	0.379	40%	0.531
Collector Assembly	0.067	40%	0.094
CFRE strut and brackets	0.977	30%	1.270
Cables to pre-amp (FCU)	0.026	30%	0.033
Pre-amplifier enclosure	0.226	30%	0.294
Pre-Amplifier	0.150	30%	0.195
Thermal Radiators	0.364	30%	0.473
Thermal System (MLI, htrs)	0.190	30%	0.247
Cables from pre-amp to SWEM	0.077	30%	0.099
SPAN Instrument	**5.888**	**22%**	**7.187**
SPAN-A Sensor Unit	**3.716**	**22%**	**4.541**
Electrostatic Analyzer	1.259	24%	1.558
Anode Assembly	0.444	16%	0.515
Electronics	1.128	20%	1.349
Miscellaneous Mechanical	0.708	26%	0.889
Thermal Blankets	0.100	30%	0.130
Cables to SWEM	0.077	30%	0.100
SPAN-B Sensor Unit	**2.172**	**22%**	**2.646**
Electrostatic Analyzer	0.656	24%	0.811
Anode Assembly	0.222	16%	0.257
Electronics	0.758	19%	0.904
Miscellaneous Mechanical	0.354	26%	0.445
Thermal Blankets	0.100	30%	0.130
Cables to SWEM	0.082	22%	0.100
SWEM	**3.036**	**27%**	**3.848**
Analog Processor (APB)	0.400	30%	0.520
High-Voltage Supply (HMB)	0.650	30%	0.845
Digital Control Board (DCB)	0.384	25%	0.480
Low-Voltage Supply (LVPS)	0.474	25%	0.593
Backplane	0.128	25%	0.160
Housing (incl connectors)	0.600	25%	0.750
Thermal System (MLI, htrs)	0.400	25%	0.500
Total Suite Mass Resources	**11.515**	**25%**	**14.448**

C Power Resource Summary

Element	CBE	Cont.	Total
	[W]	[%]	[W]
SPC Instrument	**0.250**	**38%**	**0.345**
Pre-amplifier	0.200	40%	0.280
Heaters	0.050	30%	0.065
PAN Instrument	**3.860**	**20%**	**4.632**
SPAN-A Sensor Unit	1.930	20%	2.316
SPAN-B Sensor Unit	1.930	20%	2.316
EM	**5.590**	**31%**	**7.332**
nalog Processing Board (APB)	0.7	30%	0.91
V Modulator Board (HMB)	0.85	30%	1.105
gital Control Board (DCB)	1.240	30%	1.612
w-Voltage Pwr Supply (LVPS)	2.800	30%	3.640
aters	0.050	30%	0.065
Suite Power Resources	**9.700**	**27%**	**12.309**

D ...mbly, Integration & Test (FAI&T)

E

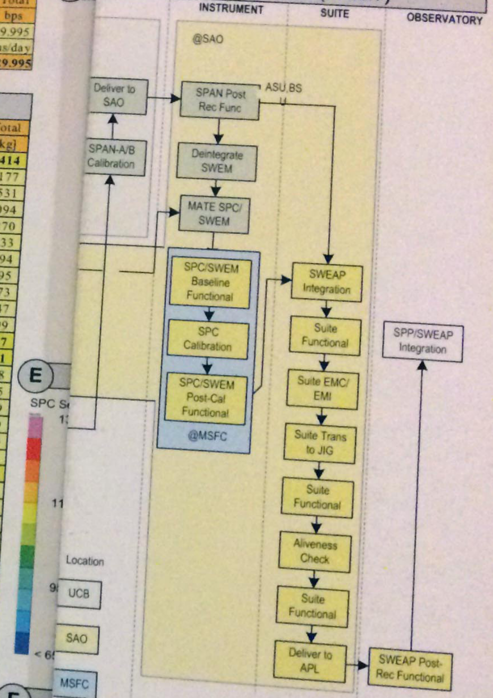

F

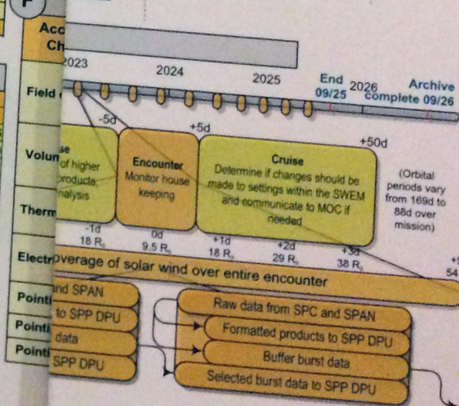

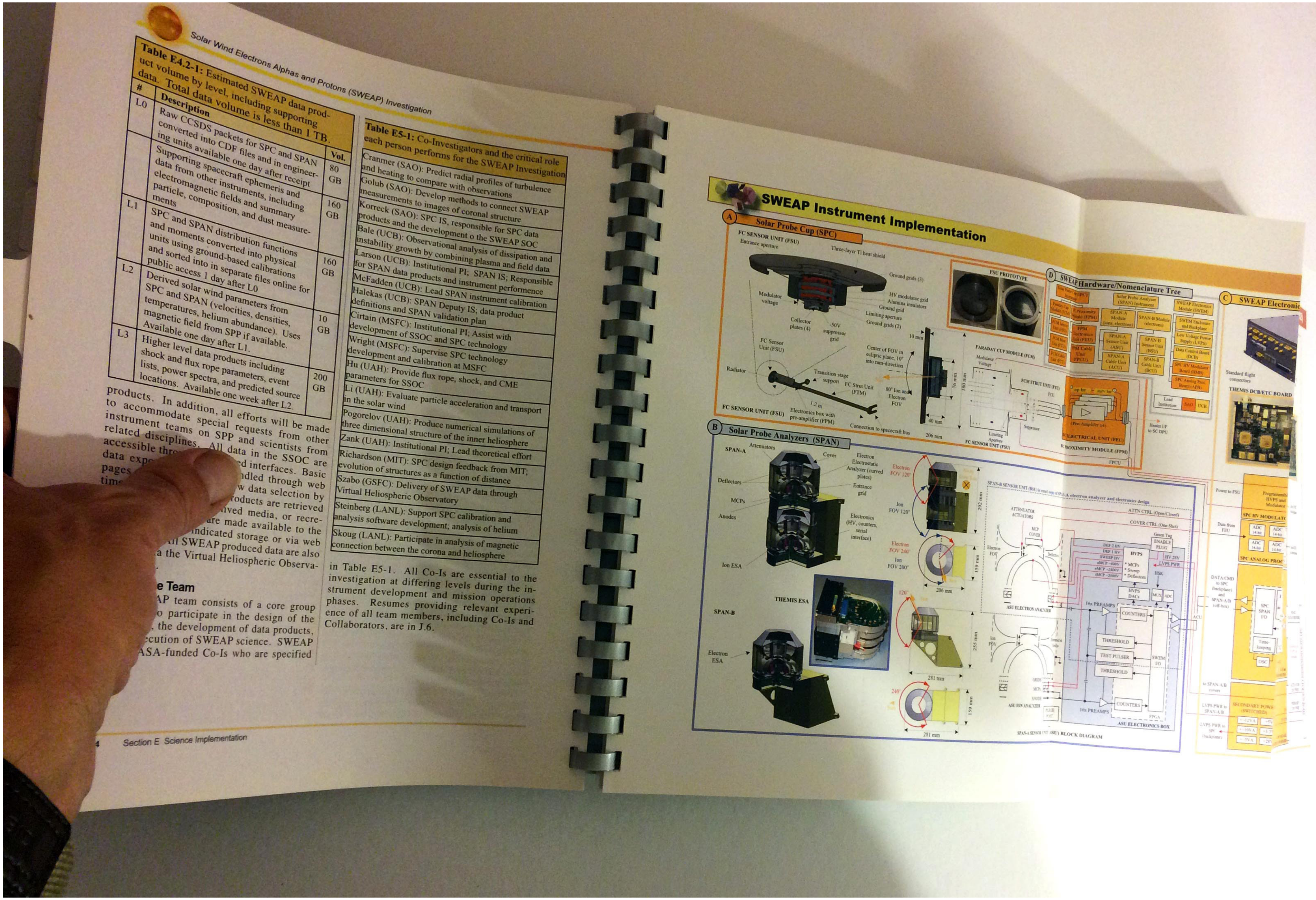

Solar Wind Electrons Alphas and Protons (SWEAP) Investigation

Table E4.2-1: Estimated SWEAP data product volume by level, including supporting data. Total data volume is less than 1 TB.

#	Description	Vol.
L0	Raw CCSDS packets for SPC and SPAN converted into CDF files and in engineering units available one day after receipt	80 GB
	Supporting spacecraft ephemeris and data from other instruments, including electromagnetic fields and summary particle, composition, and dust measurements	160 GB
L1	SPC and SPAN distribution functions and moments converted into physical units using ground-based calibrations and sorted into in separate files online for public access 1 day after L0	160 GB
L2	Derived solar wind parameters from SPC and SPAN (velocities, densities, temperatures, helium abundance). Uses magnetic field from SPP if available. Available one day after L1.	10 GB
L3	Higher level data products including shock and flux rope parameters, event lists, power spectra, and predicted source locations. Available one week after L2.	200 GB

products. In addition, all efforts will be made to accommodate special requests from other instrument teams on SPP and scientists from related disciplines. All data in the SSOC are accessible thro… data exp… …ed interfaces. Basic pages … …ndled through web tim… …w data selection by … …roducts are retrieved … …ived media, or recre… …are made available to the … …indicated storage or via web … …ll SWEAP produced data are also … …a the Virtual Heliospheric Observa-

…e Team

…AP team consists of a core group …o participate in the design of the …, the development of data products, …ecution of SWEAP science. SWEAP …ASA-funded Co-Is who are specified

Table E5-1: Co-Investigators and the critical role each person performs for the SWEAP Investigation

Cranmer (SAO): Predict radial profiles of turbulence and heating to compare with observations
Golub (SAO): Develop methods to connect SWEAP measurements to images of coronal structure
Korreck (SAO): SPC IS, responsible for SPC data products and the development o the SWEAP SOC
Bale (UCB): Observational analysis of dissipation and instability growth by combining plasma and field data
Larson (UCB): Institutional PI; SPAN IS; Responsible for SPAN data products and instrument performence
McFadden (UCB): Lead SPAN instrument calibration
Halekas (UCB): SPAN Deputy IS; data product definitions and SPAN validation plan
Cirtain (MSFC): Institutional PI; Assist with development of SSOC and SPC technology
Wright (MSFC): Supervise SPC technology development and calibration at MSFC
Hu (UAH): Provide flux rope, shock, and CME parameters for SSOC
Li (UAH): Evaluate particle acceleration and transport in the solar wind
Pogorelov (UAH): Produce numerical simulations of three dimensional structure of the inner heliosphere
Zank (UAH): Institutional PI; Lead theoretical effort
Richardson (MIT): SPC design feedback from MIT; evolution of structures as a function of distance
Szabo (GSFC): Delivery of SWEAP data through Virtual Heliospheric Observatory
Steinberg (LANL): Support SPC calibration and analysis software development; analysis of helium
Skoug (LANL): Participate in analysis of magnetic connection between the corona and heliosphere

in Table E5-1. All Co-Is are essential to the investigation at differing levels during the instrument development and mission operations phases. Resumes providing relevant experience of all team members, including Co-Is and Collaborators, are in J.6.

Section E Science Implementation

One of the several foldout sections